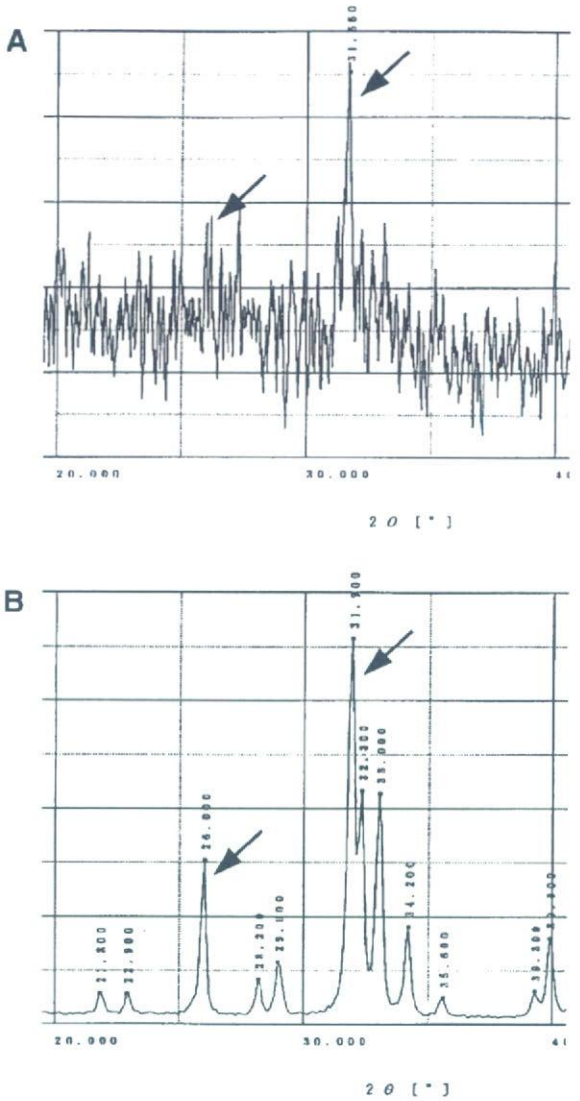

Figure 4. The powder X-ray diffraction pattern of the microcrystals synthesized by the differentiated osteoblasts on the honeycomb collagen scaffold. **A**: The X-ray diffraction spectrum demonstrated that the crystals synthesized by the osteoblasts are calcium-deficient hydroxyapatite. The lower X-ray pattern with sharp peaks (**B**) indicates a typical stoichiometric hydroxyapatite from mammalian bone. The arrows in both spectra indicate the characteristic peaks indicative of hydroxyapatite.

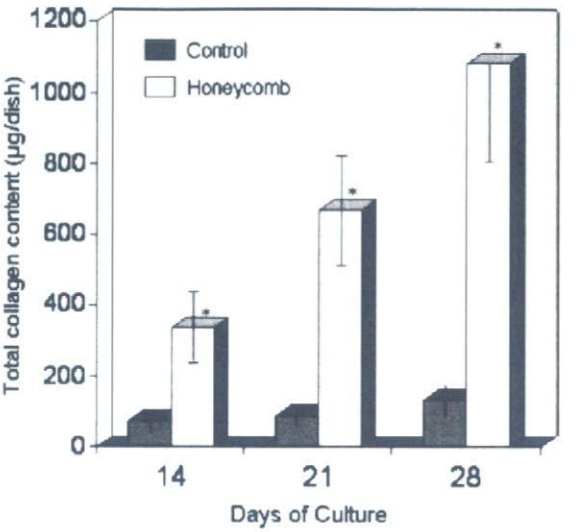

Figure 5. Total collagen content synthesized by the differentiated osteoblasts on the honeycomb collagen scaffold (*$P < 0.001$ when compared with respective controls, $n = 6$ at each time point for both control and experimental samples).

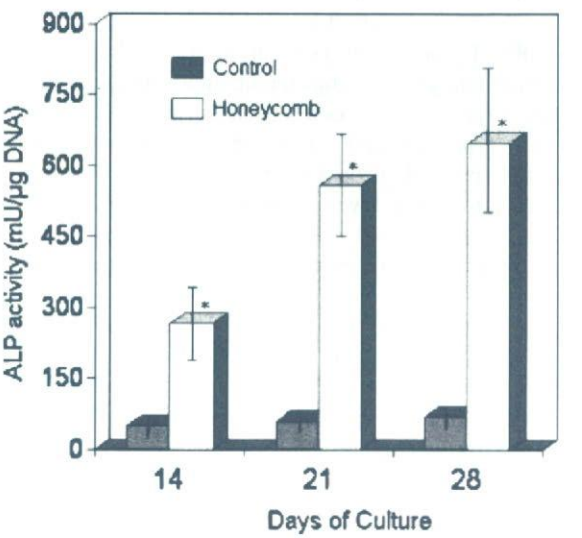

Figure 6. Alkaline phosphatase activity presented as a function of DNA during the culture of differentiated osteoblasts on a honeycomb collagen scaffold (*$P < 0.001$ when compared with respective controls, $n = 6$ at each time point for both control and experimental samples).

content on all days when compared with the respective control values. There was no significant difference in the total collagen content present in the cell harvest of control cultures without honeycomb collagen scaffold on days 21 and 28 when compared with day 14 values.

The alkaline phosphatase (ALP) activity of differentiated osteoblasts, normalized to DNA content, is illustrated in Figure 6. The alkaline phosphatase activity steadily increased in the cultures with honeycomb collagen scaffold on days 14–28. The difference was highly significant ($P < 0.001$) on all days when compared with the control cultures. About three-fold increase in the activity of ALP was observed on day 28 when compared with day 14 value. This indicated increased rates of differentiation of mesenchymal stem cells into osteoblasts in the latter periods of culture. Furthermore, the increased activity of ALP proved that the honeycomb collagen scaffolds provide an optimum environment for the normal function of osteoblasts.

DISCUSSION

Tissue engineering is emerging as a significant potential alternative to tissue or organ transplantation whereby implanted natural, synthetic, or semisynthetic tissues and

DOI 10.1002/bit

organs are used that are fully functional from the start, or that can grow into the required functionality. Collagen, the most abundant protein in the animal body is an excellent and potential biomaterial scaffold for various tissue engineering applications. In biological systems, it provides room for cell attachment, differentiation, organogenesis, tissue regeneration, and repair. Collagen is mechanically stable with high tensile strength and can be altered into different sizes and shapes with various physical and chemical modifications. The excellent tissue compatibility, decreased antigenicity and biodegradability makes collagen a major resource in biomedical, biomaterial, and tissue engineering applications.

It has been demonstrated that the unique honeycomb collagen scaffold prepared from bovine dermal atelocollagen is a suitable carrier for various 3-D cell cultures and a compatible biodegradable material in the field of tissue engineering (Masuoka et al., 2005; Sato et al., 2003). The honeycomb collagen sponge has several distinctive characteristics such as mechanical stability under various physical and chemical conditions, for the exchange of nutrients and waste products between the honeycomb membranes, and for its ability to retain its unique structure throughout the study without deformity or collapse. The pore size and thickness of the honeycomb collagen scaffold can be controlled by altering the concentrations of collagen solution and ammonia gas. This has the great advantage of creating different types of honeycomb collagen scaffolds suitable for various types of cells according to the required cell morphology and behavior. It was also reported that incorporation of a low concentration of hyaluronan in a 3-D collagen scaffold enhances matrix accumulation and cartilage specific gene expression (Allemann et al., 2001). In the present study, we demonstrated that honeycomb collagen scaffold is a suitable and biodegradable substratum for the proliferation and differentiation of rat bone marrow derived mesenchymal stem cells into osteoblasts without the presence of β-glycerophosphate and dexamethasone. The differentiated osteoblasts are capable of synthesizing the characteristic collagen and hydroxyapatite like microcrystals in culture.

Collagen is the most suitable and appropriate material for several biomaterial and biomedical applications (Lee et al., 2001; Miyata et al., 1992; Nimni, 1988; Patino et al., 2002). Various types of cells can attach, differentiate and proliferate to form a specific tissue or organ on a collagen scaffold. Different type-specific collagens may also play a role in cell attachment, differentiation, and proliferation for a particular type of cell, depending on organ or tissue of origin. Different mechanisms are involved in the attachment of cells to collagens (Rubin et al., 1981; Ruggiero et al., 1994; Schor and Court, 1979; Tandon et al., 1989). The basement membrane sulfated glycoprotein, entactin, has shown to promote cell attachment and chemotaxis (Chakravarti et al., 1990). The well-characterized arginine-glycine-aspartic (RGD) sequence is one of the major cell attachment sites in entactin and this sequence is recognized by the αvβ3 integrin receptor (Dong et al., 1995). Integrins play a major role in cell attachment and also determine how the cells interpret biochemical signals from their surrounding environment. The α1β1 and α2β1 integrins are the major collagen binding integrins, with α2β1 having a higher affinity for the fibrillar type I collagen, the major protein constituent of bone. The α2β1 integrin interaction with type I collagen is a crucial signal for the induction of osteoblastic differentiation and matrix mineralization (Mizuno and Kuboki, 2001; Mizuno et al., 2000). Furthermore, it was observed that α2β1 integrin specific collagen-mimetic surfaces supports osteoblastic differentiation (Reyes and Garcia, 2004).

The unique 3-D effects of the honeycomb scaffold may also be responsible for the attachment of mesenchymal stem cells and differentiation into osteoblasts. It was reported that the geometry of the cell scaffold is crucially important for vasculature induction and bone formation (Kuboki et al., 2001). It was also observed that honeycomb shaped hydroxyapatite tunnels, with a pore size of 300–400 μm, directly induces bone formation (Kuboki et al., 2001). In the present study, the pore size of the honeycomb collagen scaffold was within 200–400 μm, which could probably play a crucial role in the differentiation of osteoblasts. Furthermore, the wall of the honeycomb collagen scaffold may promote the attachment and deposition of autocrine cytokines and create a different environment from those of two-dimensional plastic dishes or collagen gels. Overall the 3-D cultures on a collagen scaffold provide the natural ECM environment with complex mechanical and biochemical interplay as with in living systems, which plays a vital role in the osteoblastic differentiation of mesenchymal stem cells.

Von Kossa staining and X-ray diffraction are two important tools used to examine mineralization in vitro. In the present study, staining demonstrated the formation of minerals in the osteoblast cultures with honeycomb collagen scaffold. The X-ray diffraction studies demonstrated that the microcrystals synthesized by the osteoblasts were calcium-deficient hydroxyapatite (pseudo hydroxyapatite) crystals (Fig. 5A). The X-ray patterns and the characteristic peaks correspond to those recorded for pure synthetic hydroxyapatite or mammalian bone apatite (Aoki, 1994). It is reported that bone marrow stromal cells cultured on type I collagen gel can synthesize calcified nodules in culture and can be demonstrated by Von Kossa staining and Energy-dispersive X-ray microanalysis (Hasegawa et al., 1994). Maniatopoulos et al. (1988) reported synthesis of calcium nodules in culture by rat bone marrow derived stromal cells while cultured with β-glycerophosphate and dexamethasone. The present study documented that the mesenchymal stem cells derived osteoblasts could synthesize bone-like hydroxyapatite in the presence of collagen scaffold with a unique honeycomb microenvironment.

Collagen synthesis is the primary function of differentiated osteoblasts (Koshihara and Honda, 1994). Collagen is the major constituent of bone and its unique triple helical structure provides mechanical stability for bone. In the present investigation, a steady state increase in the amount of total collagen indicated the capability of collagen synthesis

by the differentiated osteoblasts in culture. The 3-D structure and the natural ECM environment of the honeycomb collagen scaffold facilitated collagen synthesis by the differentiated osteoblasts.

Expression of alkaline phosphatase (ALP) activity is a characteristic feature of osteoblasts (Hillsley and Frangos, 1997; Rosa et al., 2003). In the present study, differentiated osteoblasts on the honeycomb collagen scaffold expressed ALP activity, which were increased to about three-fold on day 28 when compared with day 14. The increased expression of ALP activity indicated enhanced differentiation and proliferation of osteoblasts on the honeycomb collagen scaffold. In the present investigation, the cellular DNA content was increased in a steady state manner throughout the course of the study. Increase of DNA content in cell cultures was a measure of cell proliferation. In the 3-D environment on the honeycomb collagen scaffold, the cells proliferated and multiplied to a high-density manner within a short period of time, in contrast to conventional flat bed culture on dishes. This advantage of honeycomb collagen scaffold for 3-D cell cultures makes it uniquely suitable for tissue engineering applications.

Since honeycomb collagen scaffold is prepared from atelocollagen molecules, which do not contain the antigenic telopeptides, the antigenicity of atelocollagen is extremely low. Besides atelocollagen is extensively used in medical, cosmetic and tissue repair applications, with very little or no hypersensitivity reactions (DeLustro et al., 1986). It is also important that the tissue engineering scaffolds used for 3-D cell cultures should have biocompatibility and be biodegradable with little or no antigenicity (Baier Leach et al., 2003; Hutmacher, 2000). The development of an implanted tissue or organ is greatly influenced by composition, architecture and three-dimensional environment of the scaffold and its biocompatibility. The present study demonstrated that honeycomb collagen sponge is an excellent scaffold for the differentiation of mesenchymal stem cells. Using different concentrations of atelocollagen solution, it is possible to make diverse scaffolds of various sizes and shapes according to different organs or tissues such as ear, skin, liver, kidney, or cartilage. Such scaffolds can be used for 3-D cultures for specific cells either from autologous or heterologous sources. The different scaffolds prepared from atelocollagen are capable of maintaining the morphology and structural integrity, even after long-term 3-D cultures of various cells. It is important that the scaffold support the formation of bioengineered tissue that mimics the mechanical properties of the tissue or organ that is being repaired or replaced. Cells are the key unit for tissue regeneration and repair, due to their differentiation, extensive proliferation and multiplication capabilities. High-density 3-D cell cultures have enormous potential in the field of tissue engineering. The specific honeycomb structure and the porosity of the honeycomb walls allow transportation of nutrients to the cells and also for the removal of waste products. These unique advantages make honeycomb collagen scaffolds an excellent material for high-density cell cultures and their applications to cell based therapies and tissue engineering.

In conclusion, the results of the present investigation demonstrated that the honeycomb collagen sponge is an excellent scaffold for the differentiation and proliferation of mesenchymal stem cells into osteoblasts. It also proved that honeycomb collagen is an effective substrate for tissue engineering applications and may become very useful in the rapidly advancing field of stem cell technology and cell based therapy.

The authors are thankful to Professor Hideki Aoki, Tokyo Denki University, for valuable discussions and also for arranging X-ray diffraction analysis at his center.

References

Allemann F, Mizuno S, Eid K, Yates KE, Zaleske D, Glowacki J. 2001. Effects of hyaluronan on engineered articular cartilage extracellular matrix gene expression in 3-dimensional collagen scaffolds. J Biomed Mater Res 55:13–19.

Aoki H. 1994. Medical applications of hydroxyapatite. Tokyo: Ishiyaku EuroAmerica, Inc. pp 1–12.

Baier Leach J, Bivens KA, Patrick CW, Jr., Schmidt CE. 2003. Photocrosslinked hyaluronic acid hydrogels: Natural, biodegradable tissue engineering scaffolds. Biotechnol Bioeng 82:578–589.

Ballas CB, Zielske SP, Gerson SL. 2002. Adult bone marrow stem cells for cell and gene therapies: Implications for greater use. J Cell Biochem Suppl 38:20–28.

Bonewald LF, Harris SE, Rosser J, Dallas MR, Dallas SL, Camacho NP, Boyan B, Boskey A. 2003. Von Kossa staining alone is not sufficient to confirm that mineralization in vitro represents bone formation. Calcif Tissue Int 72:537–547.

Bruder SP, Fox BS. 1999. Tissue engineering of bone. Cell based strategies. Clin Orthop 367:S68–S83.

Chakravarti S, Tam MF, Chung AE. 1990. The basement membrane glycoprotein entactin promotes cell attachment and binds calcium ions. J Biol Chem 265:10597–10603.

DeLustro F, Condell RA, Nguyen MA, McPherson JM. 1986. A comparative study of the biologic and immunologic response to medical devices derived from dermal collagen. J Biomed Mater Res 20:109–120.

Dong LJ, Hsieh JC, Chung AE. 1995. Two distinct cell attachment sites in entactin are revealed by amino acid substitutions and deletion of the RGD sequence in the cysteine-rich epidermal growth factor repeat 2. J Biol Chem 270:15838–15843.

Garen A, Levinthal C. 1960. A fine-structure genetic and chemical study of the enzyme alkaline phosphatase of *E. coli* I. Purification and characterization of alkaline phosphatase. Biochim Biophys Acta 38:470–483.

Gregory CA, Prockop DJ, Spees JL. 2005. Non-hematopoietic bone marrow stem cells: Molecular control of expansion and differentiation. Exp Cell Res 306:330–335.

Hasegawa T, Oguchi H, Mizuno M, Kuboki Y. 1994. The effect of the extracellular matrix on differentiation of bone marrow stromal cells to osteoblasts. Jpn J Oral Biol 36:383–394.

Hillsley MV, Frangos JA. 1997. Alkaline phosphatase in osteoblasts is down-regulated by pulsatile fluid flow. Calcif Tissue Int 60:48–53.

Holmes TC. 2002. Novel peptide-based biomaterial scaffolds for tissue engineering. Trends Biotechnol 20:16–21.

Hutmacher DW. 2000. Scaffolds in tissue engineering bone and cartilage. Biomaterials 21:2529–2543.

DOI 10.1002/bit

Itoh H, Aso Y, Furuse M, Noishiki Y, Miyata T. 2001. A honeycomb collagen carrier for cell culture as a tissue engineering scaffold. Artif Organs 25:213–217.

Kassem M. 2004. Mesenchymal stem cells: Biological characteristics and potential clinical applications. Cloning Stem Cells 6:369–374.

Koshihara Y, Honda Y. 1994. Age-related increase in collagen production in cultured human osteoblast-like periosteal cells. Mech Ageing Dev 74:89–101.

Kuboki Y, Jin Q, Takita H. 2001. Geometry of carriers controlling phenotypic expression in BMP-induced osteogenesis and chondrogenesis. J Bone Joint Surg Am 83-A:S105–S115.

Labarca C, Paigen K. 1980. A simple, rapid, and sensitive DNA assay procedure. Anal Biochem 102:344–352.

Lee CH, Singla A, Lee Y. 2001. Biomedical applications of collagen. Int J Pharm 221:1–22.

Levenberg S, Langer R. 2004. Advances in tissue engineering. Curr Top Dev Biol 61:113–134.

Liu Tsang V, Bhatia SN. 2004. Three-dimensional tissue fabrication. Adv Drug Deliv Rev 56:1635–1647.

Maniatopoulos C, Sodek J, Melcher AH. 1988. Bone formation in vitro by stromal cells obtained from bone marrow of young adult rats. Cell Tissue Res 254:317–330.

Masuoka K, Asazuma T, Ishihara M, Sato M, Hattori H, Ishihara M, Yoshihara Y, Matsui T, Takase B, Kikuchi M, Nemoto K. 2005. Tissue engineering of articular cartilage using an allograft of cultured chondrocytes in a membrane-sealed atelocollagen honeycomb-shaped scaffold (ACHMS scaffold). J Biomed Mater Res B 75:177–184.

Mauney JR, Volloch V, Kaplan DL. 2005. Role of adult mesenchymal stem cells in bone tissue engineering applications: Current status and future prospects. Tissue Eng 11:787–802.

Miyata T, Taira T, Noishiki Y. 1992. Collagen engineering for biomaterial use. Clin Mater 9:139–148.

Mizuno M, Kuboki Y. 2001. Osteoblast-related gene expression of bone marrow cells during the osteoblastic differentiation induced by type I collagen. J Biochem (Tokyo) 129:133–138.

Mizuno M, Fujisawa R, Kuboki Y. 2000. Type I collagen-induced osteoblastic differentiation of bone-marrow cells mediated by collagen-alpha2beta1 integrin interaction. J Cell Physiol 184:207–213.

Mooney DJ, Mikos AG. 1999. Growing new organs. Sci Am 280:60–65.

Neuman RE, Logan MA. 1950. The determination of collagen and elastin in tissues. J Biol Chem 186:549–556.

Nimni ME, editor. 1988. Collagen, Vol. III. Biotechnology, Boca Raton, FL: CRC Press. pp 1–292.

Patino MG, Neiders ME, Andreana S, Noble B, Cohen RE. 2002. Collagen as an implantable material in medicine and dentistry. J Oral Implantol 28:220–225.

Pittenger MF, Mackay AM, Beck SC, Jaiswal RK, Douglas R, Mosca JD, Moorman MA, Simonetti DW, Craig S, Marshak DR. 1999. Multilineage potential of adult human mesenchymal stem cells. Science 284:143–147.

Reyes CD, Garcia AJ. 2004. Alpha2beta1 integrin-specific collagen-mimetic surfaces supporting osteoblastic differentiation. J Biomed Mater Res 69A:591–600.

Rosa AL, Beloti MM, van Noort R. 2003. Osteoblastic differentiation of cultured rat bone marrow cells on hydroxyapatite with different surface topography. Dent Mater 19:768–772.

Rubin K, Hook M, Obrink B, Timpl R. 1981. Substrate adhesion of rat hepatocytes: Mechanism of attachment to collagen substrates. Cell 24:463–470.

Ruggiero F, Champliaud MF, Garrone R, Aumailley M. 1994. Interactions between cells and collagen V molecules or single chains involve distinct mechanisms. Exp Cell Res 210:215–223.

Sato M, Asazuma T, Ishihara M, Kikuchi T, Masuoka K, Ichimura S, Kikuchi M, Kurita A, Fujikawa K. 2003. An atelocollagen honeycomb-shaped scaffold with a membrane seal (ACHMS-scaffold) for the culture of annulus fibrosus cells from an intervertebral disc. J Biomed Mater Res 64A:248–256.

Schor SL, Court J. 1979. Different mechanisms in the attachment of cells to native and denatured collagen. J Cell Sci 38:267–281.

Service RF. 2005. Tissue engineering. Technique uses body as 'bioreactor' to grow new bone. Science 309:683.

Sutherland FW, Perry TE, Yu Y, Sherwood MC, Rabkin E, Masuda Y, Garcia GA, McLellan DL, Engelmayr GC, Jr., Sacks MS, Schoen FJ, Mayer JE, Jr.. 2005. From stem cells to viable autologous semilunar heart valve. Circulation 111:2783–2791.

Tandon NN, Kralisz U, Jamieson GA. 1989. Identification of glycoprotein IV (CD36) as a primary receptor for platelet-collagen adhesion. J Biol Chem 264:7576–7583.

Woessner JF, Jr. 1961. The determination of hydroxyproline in tissue and protein samples containing small proportions of this imino acid. Arch Biochem Biophys 93:440–447.

J Artif Organs (2007) 10:212–217
DOI 10.1007/s10047-007-0391-2

ORIGINAL ARTICLE

Isao Hirata, PhD · Yuji Nomura, DDS
Manabu Ito, DDS · Atsushi Shimazu, DDS
Masayuki Okazaki, PhD

Acceleration of bone formation with BMP2 in frame-reinforced carbonate apatite–collagen sponge scaffolds

Abstract The development is expected of scaffold biomaterials that feature a shape-maintaining property in addition to high porosity and large pores that cells can easily invade. To develop a new biodegradable scaffold biomaterial reinforced with a frame, synthesized carbonate apatite (CO_3Ap) was mixed with neutralized collagen gel, and the CO_3Ap–collagen mixtures were lyophilized into sponges in a porous hydroxyapatite (HAp) frame ring. X-ray diffraction and Fourier transform infrared spectroscopy (FT-IR) analyses together with chemical analysis indicated that the synthesized CO_3Ap had a crystalline nature and a chemical composition similar to that of bone. Scanning electron microscope (SEM) observation showed that the CO_3Ap–collagen sponge had a sui pore size for cell invasion. In proliferation and differentiation experiments with osteoblasts, alkaline phosphatase and osteopontin activity were clearly detected. When these sponge–frame complexes with bone morphogenic protein (rh-BMP2) were implanted beneath the periosteum cranii of rats, significant new bone was created at the surface of the periosteum cranii after 4 weeks of implantation. These reinforced CO_3Ap–collagen sponges with rh-BMP2 are expected to be used as hard tissue scaffold biomaterials for the therapeutic purpose of the rapid cure of bone defects.

Key words CO_3apatite · Collagen sponge · Scaffold · HAp frame · BMP2

Received: March 25, 2007 / Accepted: June 19, 2007

I. Hirata · Y. Nomura · M. Okazaki (✉)
Department of Biomaterials Science, Graduate School of Biomedical Sciences, Hiroshima University, 1-2-3 Kasumi, Minami-ku, Hiroshima 734-8553, Japan
Tel. +81-82-257-5645; Fax +81-82-257-5649
e-mail: okazakix@hiroshima-u.ac.jp

M. Ito
Ishizuka Ito Dental Clinic, Yokkaichi, Japan

A. Shimazu
Department of Mucosal Immunology, Graduate School of Biomedical Sciences, Hiroshima University, Hiroshima, Japan

Introduction

A number of representative hard tissue materials have been investigated.[1–5] With the development of tissue engineering, the development of functional scaffold biomaterials is expected.[6–8] Considering the concept of biocompatibility, biodegradable materials are suitable as bioscaffolds,[9,10] and consequently we have continued to study carbonate apatite (CO_3Ap)–collagen composites. Biological apatites such as bone and teeth contain several percent of CO_3^{2-} ions,[11] so we synthesized various CO_3APs with different crystallinity and CO_3 contents.[12]

The CO_3Ap synthesized at 60°C was found to have a similar apatite property to that of bone, and we therefore prepared composites of CO_3Ap by mixing with collagen whose antigenicity had been removed by enzymatic treatment. These CO_3Ap–collagen composites showed good biocompatibility when implanted into the abdomen and beneath the periosteum cranii of rats.[13,14] In a previous study, we synthesized functionally graded CO_3Ap containing magnesium ($FGMgCO_3Ap$) using a gradient magnesium supply system, and successfully modified the gradational Mg^{2+} ions on the apatite crystals, which demonstrated no special functions on the surface.[15] The apatite demonstrated an acceleration effect of magnesium ions on osteoblast adhesion at the surface of the composite. Furthermore, when the composites were implanted beneath the periosteum cranii of rats, the $FGMgCO_3Ap$–collagen composite was metabolized faster than an CO_3Ap–collagen composite, and better formation of new bone and osteoblast arrangement at the interface between the composite and the periosteum cranii were observed. Composites were then implanted into the femur of rabbits. Clear bone formation with a higher degree of bone density was observed for the $FGMgCO_3Ap$–collagen composite[16]; however, the composites had no spaces in the inner bulk for cells to invade.

Much emphasis is placed on how cells can invade scaffold materials and how a three-dimensional (3D) cell culture can be established. Ohgushi et al.[17] reported that a porous hydroxyapatite (HAp) with a pore size of several hundred

micrometers is suitable for osteoblast invasion. We also successfully created a 70-wt% CO_3Ap–collagen sponge with pore sizes in the range 50–300 μm.[18] This sponge has a chemical composition and crystallinity similar to those of bone. X-ray high-resolution microtomography revealed a clear image of the 3D structure of the sponges. The porosity of 70-wt% CO_3Ap–collagen sponges was 72.6% ± 2.4% and it appeared to be a most favorable biomaterial from the viewpoint of natural bone properties. Osteoblasts could invade through the bottom of the sponge; however, the sponge material appeared to shrink during culture and during animal experiments. First, we considered ensuring adequate space in which new bone could easily form utilizing the concept of guided bone regeneration,[19] and we newly created a sponge reinforced with a porous HAp-frame.[20] Our concept is that sponge as cancellous bone and the frame as trabecular bone are hybridized according to the nature of natural bone. Bone formation was carried out on frame-reinforced CO_3Ap–collagen sponge scaffolds, after which they were implanted beneath the periosteum cranii of rats. Unfortunately, the bone formation was not sufficient. In this study, we investigated the acceleration of bone formation with bone morphogenic protein 2 (BMP2) using frame-reinforced CO_3Ap–collagen sponge scaffolds.

Materials and methods

Synthesis of CO_3Ap

CO_3Ap was synthesized at 60 ± 1°C and pH 7.4 ± 0.2. A 0.5-l solution of 100 mmol/l $Ca(CH_3COO)_2 \cdot H_2O$ and a 0.5-l solution of 60 mmol/l $NH_4H_2PO_4$ containing 60 mmol/l $(NH_4)_2CO_3$ were fed into a mechanically stirred solution of 1.3 mol/l acetate buffer. The suspension was stirred for 3 h and then kept at 25°C for 24 h. The CO_3Ap was separated by filtration, washed with distilled water, and dried at 60°C. Well-crystallized HAp was also synthesized at 60 ± 1°C in the same manner but without the carbonate.

Identification and chemical analysis

X-ray diffraction was employed to identify precipitates and estimate the degree of crystallinity. Measurements were made on an X-ray diffractometer (DX1, Shimadzu, Kyoto, Japan) with graphite-monochromatized CuK alpha radiation at 30 kV and 30 mA. Fourier transform infrared spectroscopy (FT-IR) analysis was carried out with a spectrometer (FT-IR 8400S, Shimadzu) by the diffuse reflectance method using powder samples containing CO_3Ap crystals (concentration 1 mg/100 mg KBr). Scanning electron micrographs (SEM) of CO_3Ap crystals were obtained using an SEM apparatus (S-4100, Hitachi, Tokyo, Japan).

Calcium concentrations were determined using an atomic absorption spectrophotometer (AA-6400, Shimadzu). Fifty milligrams each of CO_3Ap and HAp ($n = 5$) were dissolved completely in 0.1 N HCl solution and total phosphate concentrations were determined by UV spectrophotometry.[21]

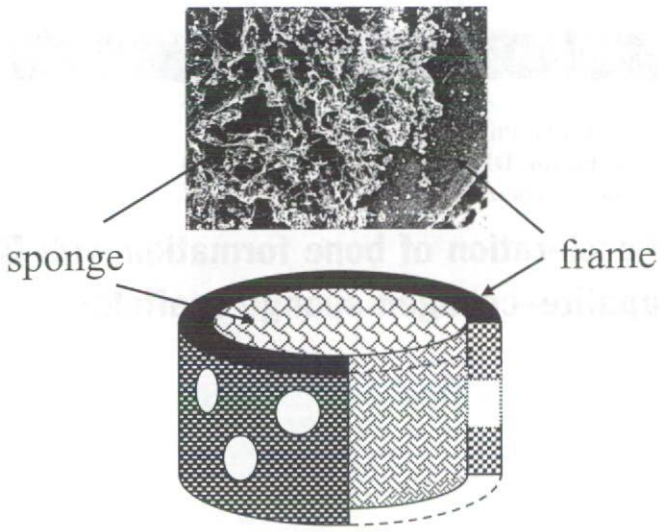

Fig. 1. Sponge reinforced with a hydroxyapatite (Hap) frame

Each 10-mg CO_3Ap sample ($n = 5$) was placed in a Conway dish and carbonate concentrations were determined by the titration method of Conway.[22]

Preparation of the frame

Sintered well-crystallized HAp powder (HAP-200, Taihei Chemicals, Nara, Japan) and paraffin wax were mixed with acetone. After evaporation of the acetone, the mixture was pressed into a mold, and a frame 7.4 mm in diameter, 2.4 mm in height, and with a thickness of 1.2 mm was formed. Then, 20 holes were opened in the side of the frame with a drill 0.6 mm in diameter. These rings were sintered at 1170°C for 2 h. The frame was shrunk onto a real frame ring 6 mm in outside diameter, 2 mm in height, and with a thickness of 1 mm, as shown in Fig. 1.

Preparation of CO3Ap–collagen sponges with frames

First, a 0.5-wt% calf skin collagen solution (Cellgen, Koken, Tokyo, Japan) was treated with enzymes to minimize its antigenicity and neutralized with 0.05 N NaOH; it was then mixed immediately with 70-wt% CO_3Ap by dry weight (70% CO_3Ap weight/sponge weight). The gels were put into each frame of a 96-well plate and then the plate was frozen at –80°C for 2 h and lyophilized in a freeze-drying machine (Eyela, Tokyo, Japan) for 24 h. The samples were subjected to UV radiation for 4 h, being placed 10 cm from the UV lamp (10 W, 253.7 nm), to become insoluble.

RNA isolation and osteoblast differentiation marker detection by reverse transcription-polymerase chain reaction

Mouse osteoblast MC3T3-E1 cells derived from untransformed mouse bone marrow were obtained from RIKEN Cell Bank (Tsukuba, Japan) and were maintained by con-

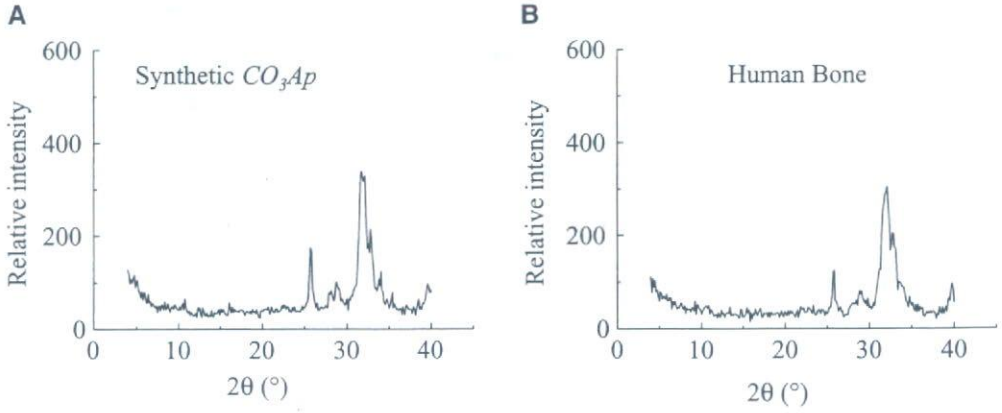

Fig. 2. X-ray diffraction pattern of synthetic carbonate apatite (CO_3Ap) (**A**) and human bone (**B**)

Table 1. Specific primers used for the polymerase chain reaction

Primer	Sequence
5′-AlPase	5′-CGG GAC TGG TAC TCG GAT AA-3′
3′-AlPase	5′-CGA AGG GTC AGT CAG GTT GT-3′
5′-OPN	5′-GAA GCT TTA CAG CCT GCA CC-3′
3′-OPN	5′-TCT CCT GGC TCT CTT TGG AA-3′
5′-GAPDH	5′-AAC TTT GGC ATT GTG GAA GG-3′
3′-GAPDH	5′-GGG TTT CTT ACT CCT TGG AG-3′

ALPase, alkaline phosphatase; OPN, osteopontin; GAPDH, glyceraldehyde-3-phosphate dehydrogenase

tinuous culture at 37°C in a 5% CO_2 humidified atmosphere. Cells were grown in Dulbecco's modified Eagle's medium (DMEM) solution supplemented with 10% heat-inactivated fetal bovine serum (FBS). Penicillin (100 U/ml) and streptomycin (100 μg/ml) were added to the media. Osteoblasts were cultured onto the CO_3Ap–collagen sponge for 10 days in α-MEM. Total RNAs were extracted with TRIzol (Invitrogen, carlsbad, CA, USA) from these osteoblasts. Aliquots of 1.0 g of total RNA were reverse transcribed using ReverTraAce (Toyobo, Osaka, Japan) with oligo(dT)20. The primers used for reverse transcription-polymerase chain reaction were designed based on the published sequence data for corresponding mouse alkaline phosphatase (ALP), osteopontin (OPN), and glyceraldehyde-3-phosphate dehydrogenase (GAPDH) (1). Amplification was performed for 1 cycle at 94°C for 2 min; 30 cycles at 94°C for 15 s, 60°C for 30 s, and 68°C for 30 s; and 1 cycle at 68°C for 4 min using KODplus polymerase (Toyobo) with the 3′- and 5′-specific primers. The polymerase chain reaction products were separated on 1% agarose gels containing ethidium bromide and were then observed on an ultraviolet transilluminator.

Animal experiments with bone morphogenic protein 2 (rh-BMP2)

The Institutional Animal Study Committee approved the study protocol of this experiment. Eight-week-old male Wistar rats (Nihon Animal, Osaka, Japan) were used. Under pentobarbital anesthesia (50 mg/kg), 60 μl of 0.1 mg/ml recombinant human bone morphogenic protein 2 (rh-BMP2) (Peprotech, Tokyo, Japan) was immersed into UV-irradiated CO_3Ap–collagen sponge with a frame and surgically implanted beneath the periosteum cranii. The animals were killed 4 weeks after the operation and the implants were dissected with the surrounding tissue and fixed in 4% paraformaldehyde-phosphate buffer. The specimens with the frame were dehydrated and embedded in paraffin. Sections 6 μm thick were cut, stained with hematoxylin-eosin, and examined under a microscope (BZ8000, Keyence, Tokyo, Japan). For low magnification, four photos were combined into one photo using a computer attached to the microscope.

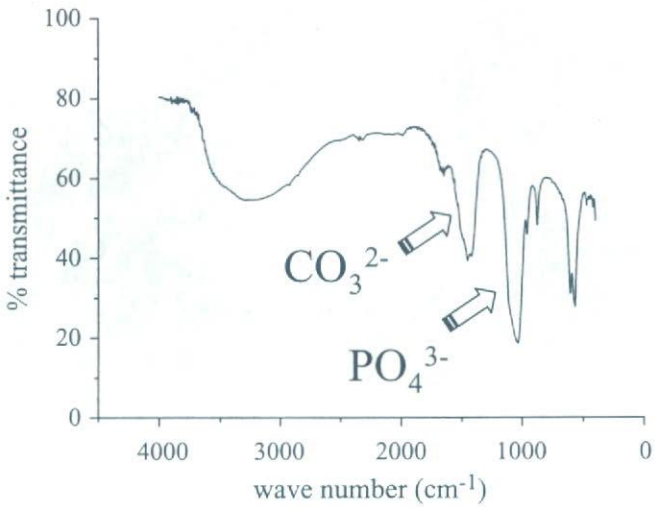

Fig. 3. Fourier transform infrared spectroscopy (FT-IR) spectrum of CO_3Ap

Results

Synthetic CO_3Ap (Fig. 2) had a poorly crystallized apatitic pattern similar to that of human bone (composition Ca, 8.94 ± 0.04 mmol/g; total P, 5.13 ± 0.10 mmol/g; and CO_3, 0.69 ± 0.05 mmol/g) compared with that of well-crystallized HAp synthesized at 60°C. FT-IR analysis of CO_3Ap showed a large adsorption band due to PO_4^{3-} at 1100–1000 cm^{-1} and a relatively small but clear adsorption band due to substituted CO_3^{2-} or adsorbed CO_2 at 1460–1410 cm^{-1} (Fig. 3).

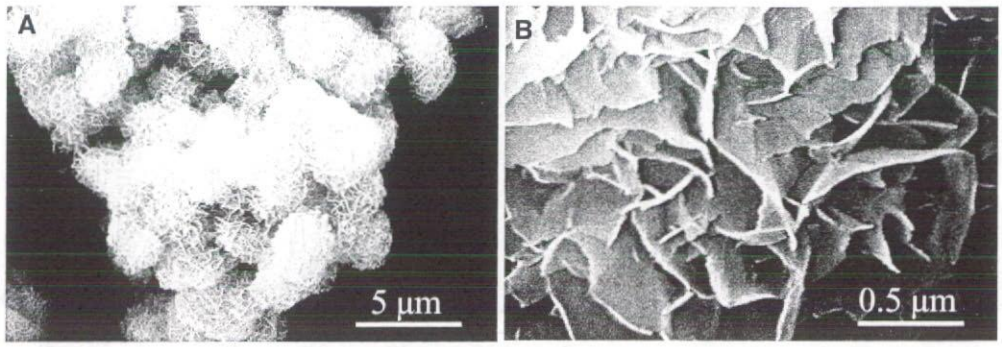

Fig. 4. Scanning electron microscope (SEM) photo of CO_3Ap crystals at two levels of magnification

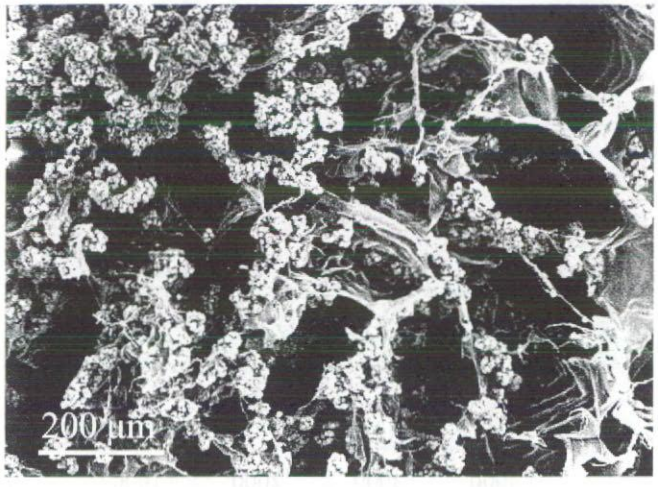

Fig. 5. SEM photo of 70-wt% CO_3Ap–collagen sponge

Figure 4A shows a scanning electron micrograph of CO_3Ap crystals, which coagulated with each other. High magnification of these CO_3Ap crystals revealed flakelike features (Fig. 4B). A CO_3Ap–collagen sponge is shown in Fig. 5, with pore sizes that are favorable for cell invasion; in general, large pores of several hundred micrometers are required for cell invasion. After 10 days of culture with osteoblasts, extracellular matrix covered the CO_3Ap–collagen sponge and the osteoblasts (Fig. 6A). ALP and OPN activity were observed on electrophoresis analysis by polymerase chain reaction (Fig. 6B). This result confirmed the mineralization activity of osteoblasts.

Figure 7 shows hematoxylin-eosin-stained CO_3Ap–collagen sponges reinforced with a porous HAp frame and injected with rh-BMP that had been implanted beneath the periosteum cranii of rats. Active bone formation was observed after 4 weeks of implantation (Fig. 7A), although sponge samples reinforced with the HAp frame without rh-BMP2 did not show adequate bone formation in a previous study.[20] Furthermore, new bone formation occurred even outside the area of the sample through the hole in the frame. At high magnification, it was observed that the newly created bone in the sponge area was strongly connected with the periosteum cranii (Fig. 7B).

Discussion

The CO_3Ap used in this study was poorly crystallized and had a CO_3 content similar to that of bone. It was concluded that the CO_3^{2-} ions were mostly substituted at the PO_4^{3-} position, on considering the previous X-ray diffraction study[12,23,24] and the chemical analysis and FT-IR analysis in this study (Fig. 3). These CO_3Ap crystals are thought to become a source element in addition to the main Ca and P elements when bone formation occurs. Poorly crystallized CO_3Ap crystals are soluble and easily metabolized during osteoclast and osteoblast activity.

The CO_3Ap–collagen sponge had sufficient space for cells to invade. The pore sizes of the sponge were approximately 50–300 μm, much larger than the size of the cells, which is around 10 μm. Osteoblasts expanded their projections and adhered to the surrounding matrix.[25,26] Furthermore, the osteoblasts secreted the collagen matrix themselves. Therefore, the invasion of osteoblasts into the deeper areas of the sponge bulk was not easy. In addition, the sponge tended to shrink in solution. Fortunately, the problem of sponge shrinkage was resolved by reinforcement with a porous frame and sponge packing. Osteoblasts could invade toward the inner part of the sponge scaffold.[20] Sponge collagen was bonded mechanically to the holes of the frame by an anchor-locking effect in addition to the chemical bond between collagen and HAp. Sponge packing was necessary to prevent sponge shrinkage in addition to the porous frame. However, since this HAp frame is not biodegradable, further investigation is in progress to produce a biodegradable CO_3Ap frame.

The effect of scaffold materials on the proliferation and differentiation of osteoblasts is important. ALP and OPN activity are useful indices of bone mineralization. The osteoblasts cultured on the CO_3Ap–collagen sponge scaffold adopted in this study showed adequate ALP and OPN activity.

In general, bone formation beneath the periosteum cranii is not so active. In fact, our previous study with a CO_3Ap–collagen composite[13,14] or sponge without cytokines did not show adequate bone formation,[18] although the CO_3Ap–collagen composites were sufficiently biocompatible. Many cytokines have been investigated and Urist[27] first discovered bone morphogenic proteins (BMPs). Later,

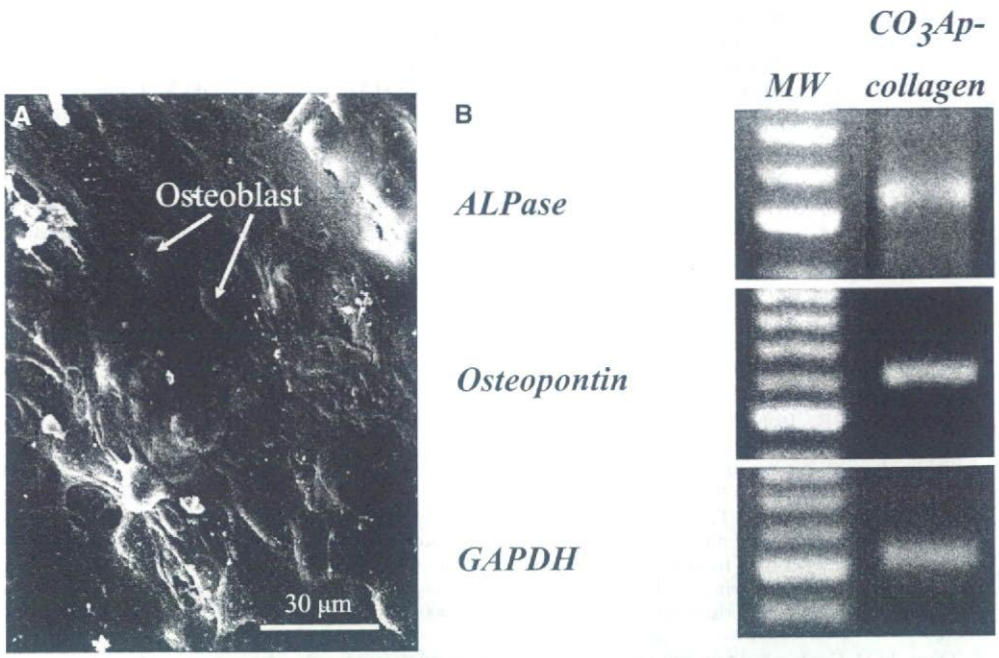

Fig. 6. SEM photo of osteoblast-like cells on the surface of a 70-wt% CO_3Ap–collagen sponge after 10 days of culture (**A**), and alkaline phosphatase (*ALP*) and osteopontin activity observed on electrophoresis analysis by polymerase chain reaction (**B**). *MW*, molecular weight; *GAPDH*, glyceraldehyde-3-phosphate dehydrogenase

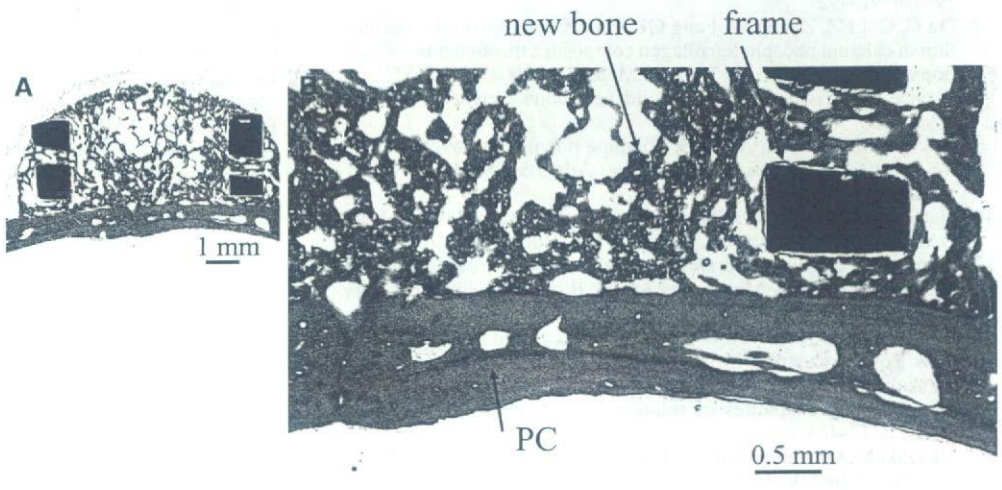

Fig. 7. Hematoxylin-eosin staining of newly created bone with 70-wt% CO_3Ap–collagen sponge reinforced with a HAp frame implanted onto the periosteum cranii (*PC*) of rats at two levels of magnification

it was identified that this BMP was BMP2, which dramatically accelerates bone formation. In addition to BMP2, various cytokines such as BMP7 were found: BMP is a kind of fibroblast growth factor (FGF). Recently, some cytokines have been commercialized; the rh-BMP2 used in this study is also sold by Peprotech.

On the other hand, some researchers purify BMP themselves. Furthermore, mesenchymal stem cells derived from adult marrow, termed multipotent adult progenitor cells, or MAPCs, were recently isolated from murine bone marrow[28]; however, the usage of stem cells requires a supply of bone marrow from the patient and time for the proliferation culture, whereas BMP combined with scaffold biomaterials needs no additional materials or techniques. Therefore, the combination of biomaterials and cytokines such as BMP is very useful for hard tissue regeneration.

Bone formation beneath the periosteum cranii has a benefit in animal experiments because this region seems to be generally inactive and thus it is difficult to form bone in this position when compared with cancellous skeletal bone. Therefore, if bone formation occurs on the periosteum cranii, it can be estimated that much more bone will be formed in other skeletal regions. In this study, more than enough bone was formed by adding rh-BMP2 in relatively short-term implantation, i.e., 4 weeks of implantation, although bone formation without rh-BMP2 required 8 weeks of implantation in a previous study.[20]

Conclusion

Cytokines, such as the rh-BMP2 used in this study, are very useful and effective for the rapid repair of bone on combination with CO_3Ap–collagen sponge as a scaffold biomaterial.

Acknowledgments This study was supported in part by Grants-in-Aid for Scientific Research No. 14370634, 15659465, and 18390515 from the Ministry of Education, Science, Sports and Culture of Japan We thank Mr. H. Minagi, Toyo Kohan Co. Ltd., Japan, for his help during HAp frame preparation, and Dr. A. Sasaki for her technical support in the animal experiments.

References

1. Nery EB, Lynch KL, Hirthe WM, Mueller KH. Bioceramic implant in surgically produced infrabony defects. J Periodontol 1975;46: 328–347
2. Ten Huisen KS, Brown PW. The formation of hydroxyapatite–gelatin composites at 38°C. J Biomed Mater Res 1994;28:27–33
3. Constantz BR, Ison IC, Fulmer MT, Poser RD, Smith ST, VanWagoner M, Ross J, Goldstein SA , Jupiter JB, Rosenthal DI. Skeletal repair by in situ formation of the mineral phase of bone. Science 1995;267:1796–1799
4. Tanahashi M, Kokubo T, Nakamura T, Katsura Y, Nagano M. Ultrastructural study of an apatite layer formed by a biomimetic process and its bonding to bone. Biomaterials 1996;17:47–51
5. Zheng X, Huang M, Ding C. Bond strength of plasma-sprayed hydroxyapatite/Ti composite coatings. Biomaterials 2000;21:841–849
6. Ohgushi H, Caplan A. Stem cell technology and bioceramics: from cell to gene engineering. J Biomed Mater Res (Appl Biomater) 1999;48:913–927
7. Du C, Cui FZ, Zhang W, Feng QL, Zhu XD, de Groot K. Formation of calcium phosphate/collagen composites through mineralization of collagen matrix. J Biomed Mater Res 2000;50:518–527
8. Service RF. Tissue engineers build new bone. Science 2000;289: 1498–1500
9. Bokhari M, Birch M, Akay G. Polyhipe polymer: a novel scaffold for in vitro bone tissue engineering. Adv Exp Med Biol 2003; 534:247–254
10. Hattori H, Masuoka K, Sato M, Ishihara M, Asazuma T, Takase B, Kikuchi M, Nemoto K, Ishihara M. Bone formation using human adipose tissue-derived stromal cells and a biodegradable scaffold. J Biomed Mater Res (Appl Biomater) 2006;76B:230–239
11. Miles AEW. Structural and chemical organization of teeth, vol II. New York: Academic, 1967
12. Okazaki M, Moriwaki Y, Aoba T, Doi Y, Takahashi J. Solubility behavior of CO_3apatites in relation to crystallinity. Caries Res 1981;15:477–483
13. Okazaki M, Ohmae H, Hino T. Insolubilization of apatite–collagen composites by UV irradiation. Biomaterials 1989;10:564–568
14. Okazaki M, Ohmae H, Takahashi J, Kimura H, Sakuda M. Insolubilized properties of UV-irradiated CO_3apatite–collagen composites. Biomaterials 1990;11:568–572
15. Yamasaki Y, Yoshida Y, Okazaki M, Shimazu A, Uchida T, Kubo T, Akagawa Y, Hamada Y, Takahashi J, Matsuura N. Synthesis of functionally graded $MgCO_3$apatite accelerating osteoblast adhesion. J Biomed Mater Res 2002;62:99–105
16. Yamasaki Y, Yoshida Y, Okazaki M, Shimazu A, Kubo T, Akagawa Y, Uchida T. Action of FG$MgCO_3$Ap–collagen composite in promoting bone formation. Biomaterials 2003;24:4913–4920
17. Ohgushi H, Goldberg VM, Caplan AI. Heterotopic osteogenesis in porous ceramics induced by marrow cells. J Orthop Res 1989; 7:568–578
18. Itoh M, Shimazu A, Hirata I, Yoshida Y, Shintani H, Okazaki M. Characterization of CO_3Ap–collagen sponges using X-ray high-resolution microtomography. Biomaterials 2004;25:2577–2583
19. Ignatius AA, Ohnmacht M, Claes LE, Kreidler JP, Palm F. A composite polymer/tricalcium phosphate membrane for guided bone regeneration in maxillofacial surgery. J Biomed Mater Res 2001;58:564–569
20. Tieliewuhan Y, Hirata I, Sasaki A, Minagi H, Okazaki M. Osteoblast proliferation behavior and bone formation on and in CO_3apatite-collagen sponges reinforced with a porous hydroxyapatite frame. Dent Mater J 2004;23:258–264
21. Eastoe JE. Method for the determination of phosphate calcium and protein in small portions of mineralized tissues. Liege: University of Liege, 1965
22. Conway EJ. Microdiffusion analysis and volumetric error. 3rd ed. New York: Van Nostrand, 1950
23. LeGeros RZ. Apatites from aqueous and nonaqueous systems: relation to biological apatites. Proceedings of First International Congress on Phosphorus Compounds, Rabat, 1977;347–360
24. LeGeros RZ. Calcium phosphates in oral biology and medicine: Monographs in oral science, vol 15 (Myers HM, series editor). Basel: Karger, 1991
25. Albert B, Bray D, Lewis J, Raff M, Roberts K, Watson JD. Molecular biology of the cell. 3rd ed. New York: Garland, 1994
26. Hirata I, Nomura Y, Tabata H, Miake Y, Yanagisawa T, Okazaki M. SEM observation of collagen fibrils secreted from the body surface of osteoblasts on a CO_3apatite–collagen sponge. Dent Mater J 2005;24:460–464
27. Urist MR. Bone: formation by autoinduction. Science 1965;150: 893–899
28. Jiang Y, Jahagirdar BN, Reinhardt RL, Schwartz RE, Keene CD, Ortiz-Gonzalez XR, Reyes M, Lenvik T, Lund T, Blackstad M, Du J, Aldrich S, Lisberg A, Low WC, Largaespada DA, Verfaillie CM. Pluripotency of mesenchymal stem cells derived from adult marrow. Nature 2002;418:41–49

J Mater Sci: Mater Med (2007) 18:1361–1367
DOI 10.1007/s10856-007-0123-4

Fabrication of porous low crystalline calcite block by carbonation of calcium hydroxide compact

Shigeki Matsuya · Xin Lin · Koh-ichi Udoh · Masaharu Nakagawa · Ryoji Shimogoryo · Yoshihiro Terada · Kunio Ishikawa

Received: 24 June 2005 / Accepted: 3 March 2006 / Published online: 3 February 2007

Abstract Calcium carbonate ($CaCO_3$) has been widely used as a bone substitute material because of its excellent tissue response and good resorbability. In this experimental study, we propose a new method obtaining porous $CaCO_3$ monolith for an artificial bone substitute. In the method, calcium hydroxide compacts were exposed to carbon dioxide saturated with water vapor at room temperature. Carbonation completed within 3 days and calcite was the only product. The mechanical strength of $CaCO_3$ monolith increased with carbonation period and molding pressure. Development of mechanical strength proceeded through two steps; the first rapid increase by bonding with calcite layer formed at the surface of calcium hydroxide particles and the latter increase by the full conversion of calcium hydroxide to calcite. The latter process was thought to be controlled by the diffusion of CO_2 through micropores in the surface calcite layer. Porosity of calcite blocks thus prepared had 36.8–48.1% depending on molding pressure between 1 MPa and 5 MPa. We concluded that the present method may be useful for the preparation of bone substitutes or the preparation of source material for bone substitutes since this method succeeded in fabricating a low-crystalline, and thus a highly reactive, porous calcite block.

S. Matsuya (✉)
Section of Bioengineering, Department of Dental Engineering, Fukuoka Dental College, 2-15-1 Tamura, Sawara-ku, Fukuoka 814-0193, Japan
e-mail: smatsuya@college.fdcnet.ac.jp

X. Lin · M. Nakagawa · R. Shimogoryo · K. Ishikawa
Department of Biomaterials, Faculty of Dental Science, Kyushu University, 3-3-1 Maidashi, Higashi-ku, Fukuoka 812-8582, Japan

K. Udoh
Institute of Biochemical Research and Education, School of Medicine, Yamaguchi University, 1-1-1 Minamiogushi, Yamaguchi 755-8505, Japan

X. Lin · Y. Terada
Department of Fixed Prosthodontics, Faculty of Dental Science, Kyushu University, Higashi-ku, Fukuoka 812-8582, Japan

R. Shimogoryo
Japan Institute for Advanced Dentistry, Shiba TK Building 4F, 1-8-25, Shiba, Minatoku, Tokyo 105-0014, Japan

Introduction

Calcium carbonate ($CaCO_3$) plays an important role in the reconstruction of bone defects as bone filler or as a source material for bone fillers. A typical example is the marine coral. Marine coral is made of aragonite-type $CaCO_3$ (97%<), and its skeleton with a porous microstructure is morphologically quite similar to that of human cancellous bone. The coral has been clinically used as bone substitute in dental, maxillo-facial, cranio-facial, and orthopedic surgeries for the reconstruction of bone defects [1–5]. When implanted in bone defect, it does not cause inflammatory response, shows excellent tissue response, and is gradually resorbed with time. The marine coral is also used as a source material to prepare apatite-type bone fillers. When the coral is hydrothermally treated in the presence of phosphate salts, it transforms into apatitic mineral without changing its morphology. The bone filler is called coralline apatite and has been widely used as a bone substitute in the United States [6–8].

Although the coral has some ideal characteristics as bone filler or as a source material for bone fillers, there are some drawbacks. For example, the coral suitable for bone filler can only be found in and collected from the ocean. Therefore, it costs much and is now much criticized since it destroys nature. Moreover, collected corals have to be cleaned to prevent inflammatory reaction caused by proteins and other elements present as impurities.

Drawbacks of the coral mentioned above would be solved if $CaCO_3$ block can be prepared artificially. One of the methods to prepare pure $CaCO_3$ block is the sintering of $CaCO_3$ powder. However, sintering process causes liberation of carbon dioxide and leads to calcium oxide formation. In addition, $CaCO_3$ with extremely high crystallinity is obtained even when low crystalline $CaCO_3$ powder is used. Unfortunately, formation of calcium oxide and high-crystalline $CaCO_3$ is not desirable with respect to tissue response and resorbability. On the other hand, calcium hydroxide ($Ca(OH)_2$) is well known as a non-hydraulic cement in the fields of cement and concrete. When $Ca(OH)_2$ is exposed to carbon dioxide that exists in air, $Ca(OH)_2$ hardens and forms $CaCO_3$ [9–12]. However, to date, there are no reports on how to fabricate $CaCO_3$ block aimed for the reconstruction of bone defects based on carbonation of calcium hydroxide. In the present study, therefore, we investigated the reaction process between $Ca(OH)_2$ compact and CO_2 gas, and evaluated the feasibility of $CaCO_3$ block preparation based on the carbonation reaction.

Materials and methods

Calcium hydroxide compact preparation

Commercially available calcium hydroxide ($Ca(OH)_2$; Nacalai Tesque, Kyoto, Japan) was used in this study. The $Ca(OH)_2$ powder, 0.2 g, was placed in a stainless steel mold and pressed uniaxially with an oil pressure press machine (Riken Power, Riken Seiki, Japan) under 1–5 MPa pressure. Specimens prepared were 10 mm in diameter and 1–3 mm in thickness. In a similar way, column compacts of 6 mm in diameter and 11–13 mm in height were also prepared using another stainless steel mold.

Carbonation of $Ca(OH)_2$ compact

$Ca(OH)_2$ compacts were placed in carbon dioxide reaction vessel for 1–72 h at room temperature for carbonation. The reaction vessel—approximately 5 L—was saturated with water vapor, and carbon dioxide gas was supplied at a rate of 0.15–0.20 L/min.

Mechanical testing

Mechanical strength of the specimens was evaluated in terms of diametral tensile strength (DTS) and compressive strength (CS) at room temperature at a constant cross-head speed of 1 mm/min on a universal testing machine (IS5000, Shimadzu, Kyoto, Japan). At least five specimens were used for each condition.

X-ray diffraction analysis

The specimens were ground into fine powders and characterized by powder X-ray diffraction (XRD) analysis. The XRD patterns of the specimens were recorded with a vertically mounted diffractometer system (RINT 2500V, Rigaku, Tokyo, Japan) using counter-monochromatized CuK_α radiation generated at 40 kV and 100 mA. The specimens were scanned from 10° to 60° 2θ in a continuous mode at a scanning rate of 2°/min. Quantitative analysis was also done on the specimens during carbonation. Calibration curve for the quantitative analysis was made using separated diffraction peaks of $Ca(OH)_2$ (001, d = 4.905 Å) and calcite (0-22, d = 2.095 Å) respectively.

Microstructure

Morphology of the surfaces and fracture surfaces of the specimens was characterized by means of a scanning electron microscope (SEM; JSM 5400LV, JEOL, Tokyo, Japan) at an acceleration voltage of 15 kV after gold coating.

Porosity measurement

The apparent density of specimen was calculated from specimen's weight and dimensions. Relative density was calculated from the ratio of apparent density over the theoretical density of calcite (2.711 g/cm^3). The total porosity of specimen is then defined as

$$\text{Total porosity}\,(\%) = 100\,(\%) - \text{Relative density}\,(\%)$$

Total porosity was the average value of at least five specimens.

Results and discussion

No obvious morphological changes were observed macroscopically even when the $Ca(OH)_2$ compact

was exposed to carbon dioxide up to 72 h (data not shown).

Figure 1 shows the typical SEM photographs of the surfaces and fracture surfaces before and after carbonation for 1–72 h when $Ca(OH)_2$ was compacted under a pressure of 1 MPa. The original $Ca(OH)_2$ powder had particle size ranging from sub micron to several microns with irregular shape. As shown in Fig. 1, we found no remarkable differences before and after the carbonation process or at the time of carbonation—even at SEM level.

Figure 2 shows the typical SEM photographs of the fracture surfaces of $Ca(OH)_2$ compacts prepared at various molding pressures between 1 MPa and 5 MPa after carbonation for 72 h. Basically, less pores and smaller pores were observed in the $Ca(OH)_2$ compact prepared at higher pressure.

Table 1 summarizes the porosity of $Ca(OH)_2$ compact when exposed to carbon dioxide for 72 h. As shown in Table 1, the porosity decreased with increase in molding pressure.

Figure 3 shows the change in powder XRD pattern of $Ca(OH)_2$ compact prepared at 2 MPa for a carbonation duration of 0–72 h. As shown in Fig. 3, $Ca(OH)_2$ transformed directly to $CaCO_3$ with time even though no morphological changes were observed with SEM. Carbonation was almost complete at 72 h. It was also shown that the $CaCO_3$ formed was calcite—which is the most stable phase among all $CaCO_3$ modifications. It has been reported that the biological properties of calcite are almost the same as those of aragonite, which is a constituent of marine coral [13]. Therefore, this calcite block is expected to show similar tissue response with marine coral if other factors, including

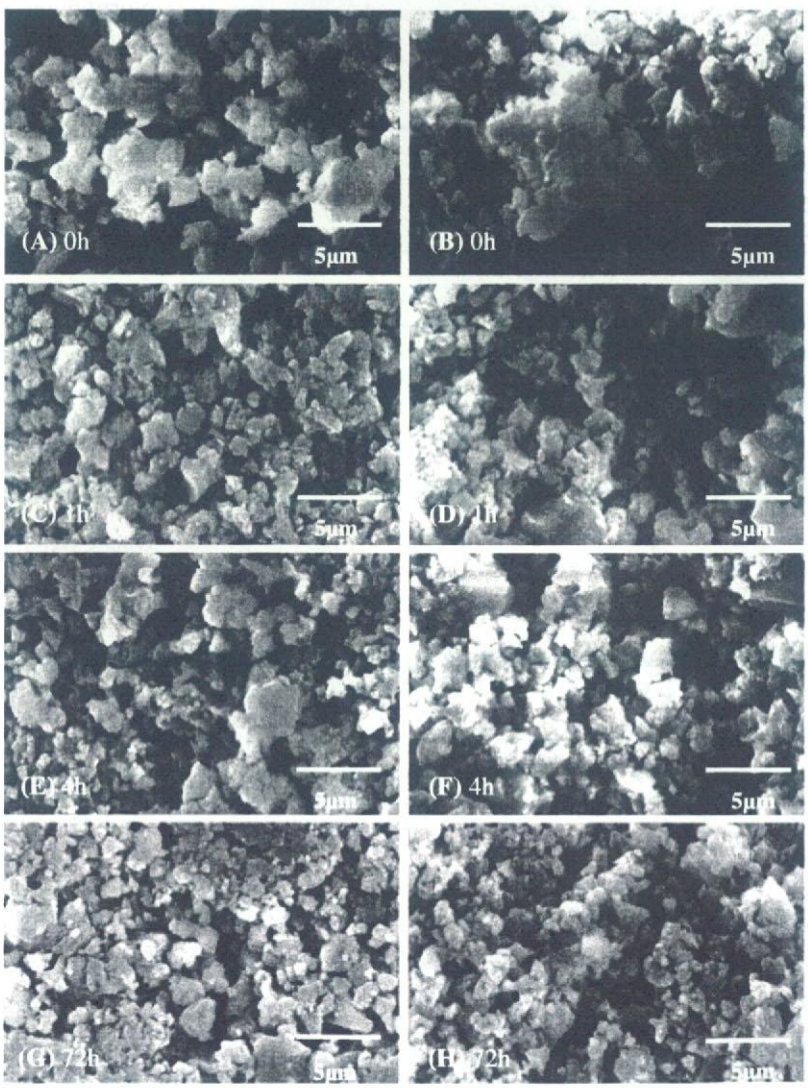

Fig. 1 Scanning electron microscopic observation of the surfaces and fracture surfaces of calcium hydroxide compacts under a pressure of 1 Mpa. (**A** and **B**) Before carbonation. (**C** and **D**) Carbonated for 1 h (**E** and **F**) Carbonated for 4 h (**G** and **H**) Carbonated for 72 h (**A**, **C**, **E** and **G**) Surfaces (**B**, **D**, **F** and **H**) Fracture surfaces

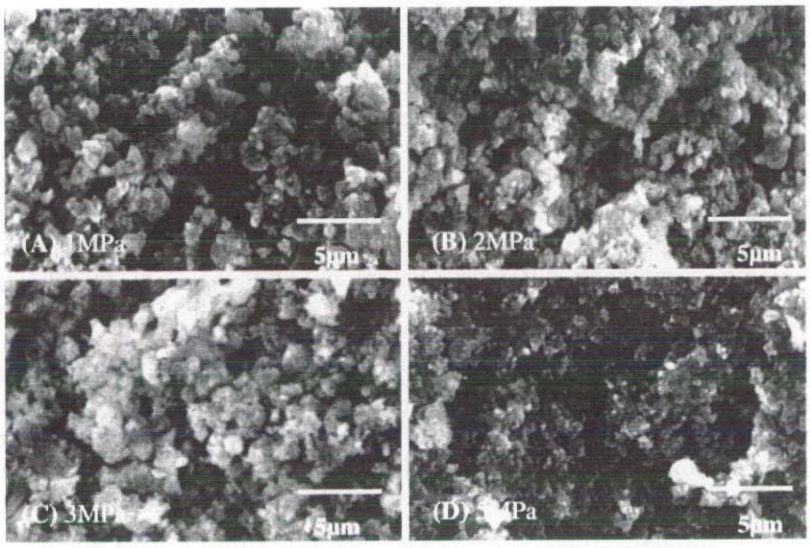

Fig. 2 Scanning electron microscopic observation of the fracture surfaces of calcium hydroxide compacts carbonated for 72 h

Table 1 Porosity of $Ca(OH)_2$ compacts when prepared at various molding pressures and carbonated for 72 h

Molding pressure (MPa)	Porosity (%)
1	48.1 ± 1.0
2	42.2 ± 0.6
3	41.5 ± 1.6
5	36.8 ± 0.4

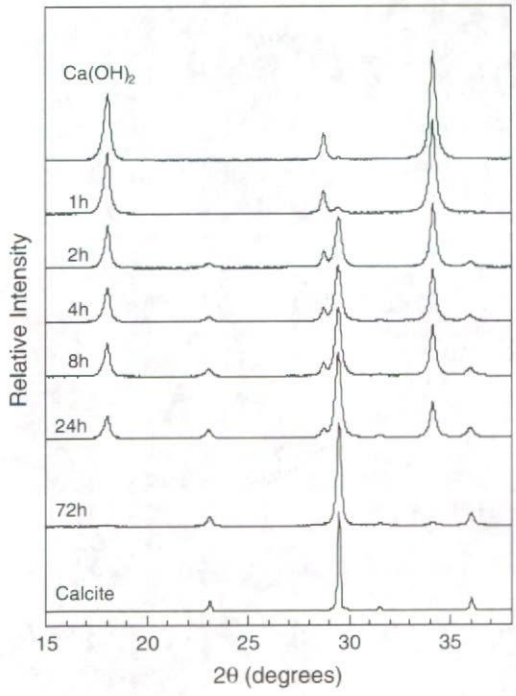

Fig. 3 Powder XRD patterns of the $Ca(OH)_2$ compacts prepared at 2 MPa during carbonation for 0–72 h

morphological ones, are the same. In the XRD pattern of the specimen, peaks broader than commercially obtained $CaCO_3$ powder were observed, indicating that the crystallite size of calcite formed by carbonation was much smaller. Crystallite size of the specimen was estimated as 262–306 nm, whereas that of a commercial $CaCO_3$ powder was 834 nm. The small crystallite size may be the reason why no morphological changes were observed at SEM level even though $Ca(OH)_2$ had transformed to calcite. For $Ca(OH)_2$ compacts prepared at other molding pressures, the changes in XRD patterns were similar to that in Fig. 3 (data not shown).

Figure 4 shows the change with time in the amount of $Ca(OH)_2$ and calcite phase in compacts subject to different molding pressures. As shown in Fig. 4, the transformation of $Ca(OH)_2$ to calcite proceeded in two stages. At the first stage within 2–4 h, transformation

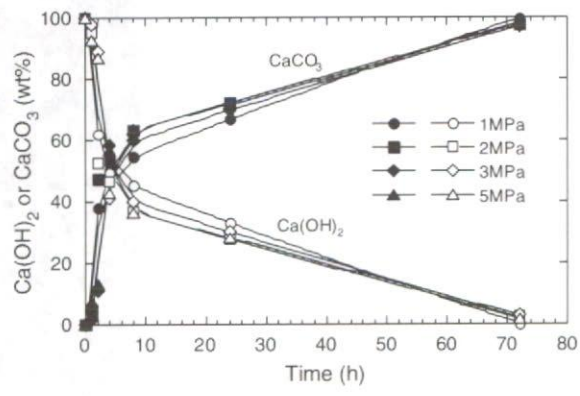

Fig. 4 Changes in the amount of $Ca(OH)_2$ and calcite phase in the compacts with time at various molding pressures

was very rapid such that approximately 50% of $Ca(OH)_2$ was converted to calcite. At the second stage, rate of transformation was much slower when compared to the first stage, and the remaining $Ca(OH)_2$ was transformed to calcite during this stage. Basically, these tendencies were the same regardless of molding pressure. When transformation rates were compared based on molding pressure, specimens molded at lower pressure underwent faster transformation at the first stage. The second stage took a much longer time than the first stage, and thus the time required for the whole transformation was almost the same regardless of molding pressure. The two-stage transformation became much clearer when the amount of calcite formed was plotted against square root of time for a kinetic analysis, as shown in Fig. 5. At the second stage, a linear relation was observed between 2–4 h and 72 h regardless of molding pressure. The slopes, corresponding to diffusion coefficient, were almost the same regardless of molding pressure. Since a linear relation was observed at the second stage (where approximately 50% of $Ca(OH)_2$ was already converted to calcite at the beginning of second stage), it could thus be suggested that carbonation rate at the second stage was controlled by diffusion process through calcite layer formed initially on the surface of $Ca(OH)_2$ particles. Two candidates were proposed for the diffusion: one was CO_3^{2-} ion and the other was CO_2 gas. It was reported that the diffusion coefficient (D) of CO_3^{2-} ion for lattice diffusion in calcite was expressed by the equation, D (cm^2/s) = 0.65 exp (–56,900 cal/RT) [14]. D at room temperature (T = 298 K) is calculated as 1.2×10^{-42}, and this value led to the conclusion that the lattice diffusion of CO_3^{2-} ion in calcite was actually negligible in the condition employed in the present study. On the other hand, carbonation of CaO at high temperature was reported to be followed by the diffusion of CO_2 gas through $CaCO_3$ layer formed on the surface of CaO [11, 15]. Likewise in the present $Ca(OH)_2$ system, it could be thought that carbonation process at the second stage was controlled by the diffusion of CO_2 molecules through calcite layer formed initially on the surface of $Ca(OH)_2$ particles.

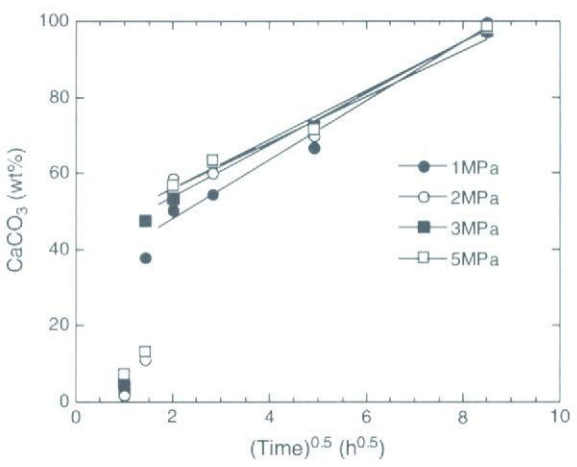

Fig. 5 Changes in the amount of calcite phase in the compacts plotted against square root of time with time at various molding pressures

Figure 6 shows the change of (a) DTS and (b) CS values of $Ca(OH)_2$ compacts prepared at different molding pressures of 1, 2, 3, and 5 MPa as a function of carbonation time. Both DTS and CS values increased with time up to 24 h regardless of molding pressure, and they remained constant after that time period. On the other hand, higher DTS and CS values were obtained for specimens prepared under higher molding pressure. Relating these results to the data in Table 1, it was thus logical to conclude that higher mechanical strength was caused by lower porosity (Table 1).

When it comes to understanding the relationship between mechanical strength and calcite formation in

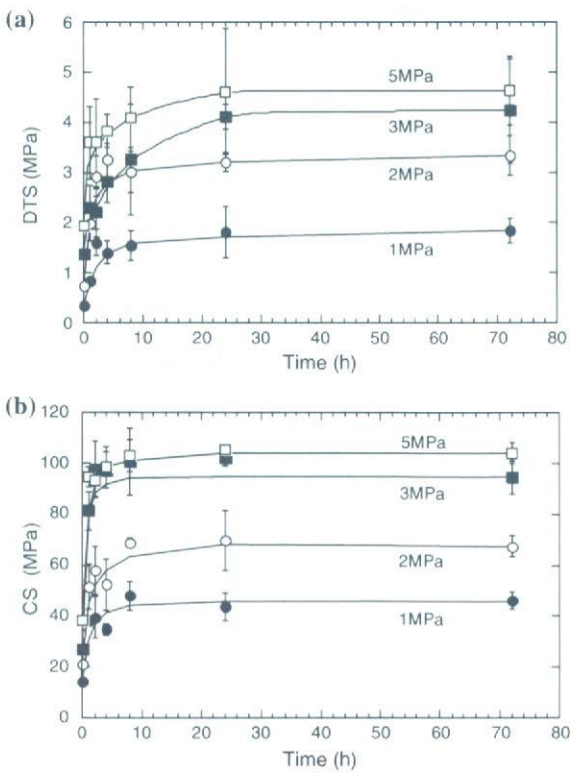

Fig. 6 (**a**) Changes in diametral tensile strength of compacts pressed at 1, 2, 3 and 5 MPa during carbonation with time. (**b**) Changes in compressive strength of column compacts pressed at 1, 2, 3 and 5 MPa during carbonation with time

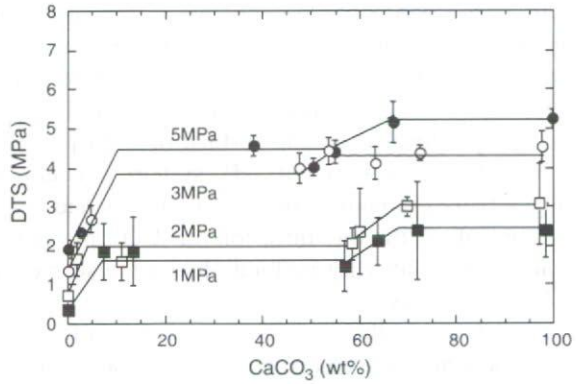

Fig. 7 Changes in DTS values of the $Ca(OH)_2$ compacts prepared at various molding pressures with the amount of formed calcite

the context of the two-stage reaction process, Fig. 7 is very helpful in that the DTS values of $Ca(OH)_2$ compacts prepared at various molding pressures were plotted against the amount of calcite formed. As shown in this figure, the increase of DTS could be divided into two stages. At the first stage, a rapid increase in DTS values was observed based on approximately 10% calcite formation. After the initial rapid increase in mechanical strength, no increase was observed until the juncture when approximately 50% of calcite was formed. Then at the second stage, mechanical strength increased again, until approximately 50–70% of calcite was formed.

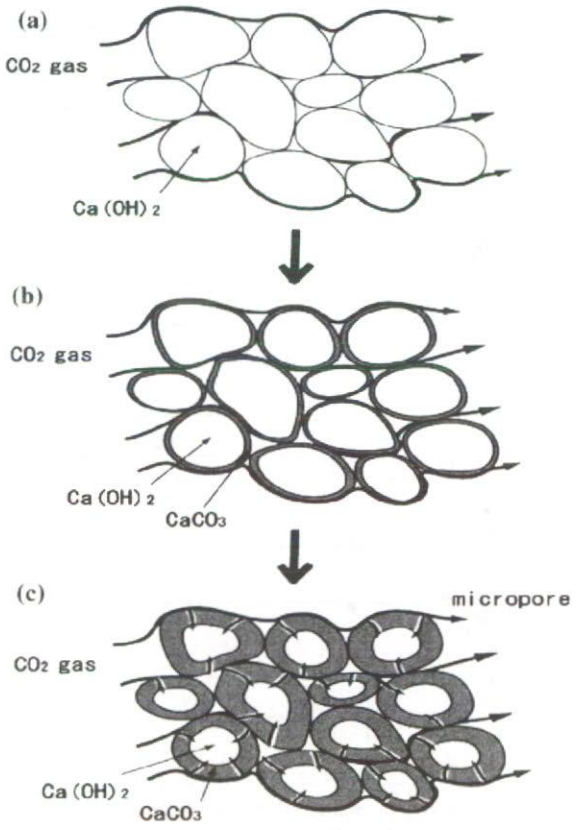

Fig. 8 The schematic model of carbonation process of $Ca(OH)_2$ when exposed to CO_2 gas

Figure 8 shows a schematic model of the carbonation process of $Ca(OH)_2$. When $Ca(OH)_2$ compact was exposed to CO_2 gas, the surface of $Ca(OH)_2$ particles was carbonated to form a calcite layer on their surface (Fig. 8a, b). This initial process was very quick since it was only a surface reaction between $Ca(OH)_2$ particles and CO_2 gas. Carbonation of the surfaces of $Ca(OH)_2$ particles then resulted in an initial rapid increase in mechanical strength whereby $Ca(OH)_2$ particles were bonded with the calcite crystals formed on the surface (Fig. 8b). At the second stage, further carbonation proceeded with time, although the rate of transformation was much slower than that of the initial stage. This was because carbonation reaction at this state was controlled by diffusion of CO_2 gas through micropores in calcite layer as shown in (Fig. 8c). Mechanical strength of the specimen was independent of the degree of carbonation process for a while since mechanical strength of calcium hydroxide governed the mechanical strength of the specimen at this carbonation ratio. When calcite formed was approximately 50%, mechanical strength developed further. This could be because mechanical strength of the specimen was governed by the amount of calcite formed at this stage, instead of calcium hydroxide.

Conclusions

We found that pure, low-crystalline porous calcite block with high mechanical strength could be prepared by exposing $Ca(OH)_2$ compact to carbon dioxide saturated with water vapor at room temperature. Although no cell test or histological evaluation was done in the present study, low crystallinity indicates higher reactivity and resorbability. Thus calcite porous block prepared in this method is expected to be useful as a bone substitute or as a source material for the fabrication of bone substitutes.

Mechanical strength development was closely related to the transformation of $Ca(OH)_2$ to calcite. Crystal morphology was the same before and after carbonation even at SEM level—which may be a good advantage for the fabrication of bone substitute blocks.

Acknowledgments This study was supported in part by a Grant-in-aid for Scientific Research from the Ministry of Education, Sports, Culture, Science, and Technology, Japan.

References

1. F. SOUYRIS, C. PELLEQUER, C. PAYROT and C. SERVERA, *J. Maxillofac. Surg.* **13**(2) (1985) 64.
2. G. GUILLEMIN, J. L. PATAT, J. FOURNIE and M. CHETAIL, *J. Biomed. Mater. Res.* **21**(5) (1987) 557.
3. J. L. PATAT and G. GUILLEMIN, *Annal. Chirurg. Plast Esthet.* **34**(3) (1989) 221.
4. F. X. ROUX, D. BRASNU, B. LOTY, B. GEORGE and G. GUILLEMIN, *J. Neurosurg.* **69**(4) (1988) 510.
5. F. X. ROUX, B. LOTY, D. BRASNU and G. GUILLEMIN, *Neuro-Chirurgie* **34**(2) (1988) 110.
6. D. M. ROY and S. K. LINNEHAN, *Nature* **247** (1974) 220.
7. M. SIVAKUMAR, T. S. KUMAR, K. I. SHANTHA and K. P. RAO, *Biomaterials* **17** (1996) 1709.
8. W. SUCHANEK and M. YOSHIMURA, *J. Mater. Res.* **13** (1998) 94.
9. O. MATSUDA and H. AMADA, *Gypsum Lime* **97** (1968) 3.
10. O. MATSUDA and H. YAMADA, *Gypsum Lime* **125** (1973) 8.
11. D. R. MOOREHEAD, *Cement Concrete Res.* **16** (1986) 700.
12. O. CAZALLA, C. RODRIGUEZ-NAVARRO, E. SEBASTIAN, G. CULTRONE and M. J. TORRE DE LA, *J. Am. Ceram. Soc.* **83** (5) (2000) 1070.
13. J. C. FRICAIN, R. BAREILLE, F. ULYSSE, B. DUPUY and J. AMDEE, *J. Biomed. Mater. Res.* **42** (1998) 96.
14. D. MESS, A. F. SAROFIM and J. P. LONGWELL, *Energy Fuels* **13** (1999) 999.
15. M. CHEN, S. ITO and A. YAMAGUCHI, *J. Ceram. Soc. Jpn.* **110** (6) (2002) 512.

Transformation of 3DP Gypsum Model to HA by Treating in Ammonium Phosphate Solution

Rungnapa Lowmunkong,[1] Taiji Sohmura,[1] Junzo Takahashi,[1] Yumiko Suzuki,[2] Shigeki Matsuya,[2] Kunio Ishikawa[2]

[1] Division of Oromaxillofacial Regeneration, Course for Integrated Oral Sciences and Stomatology, Osaka University Graduate School of Dentistry, Yamadaoka, I-8 Suita, Osaka 565-0871, Japan

[2] Faculty of Dental Science, Department of Biomaterials, Kyushu University, Maidashi, 3–1-1 Higashi-ku, Fukuoka 812-8582, Japan

Received 21 January 2005; revised 28 October 2005; accepted 9 March 2006
Published online 12 July 2006 in Wiley InterScience (www.interscience.wiley.com). DOI: 10.1002/jbm.b.30609

Abstract: Three-dimensional printing (3DP) is a CAD/CAM built-up using ink-jet printing technique. Commercially available 3DP system can form only gypsum model and not for bioceramics. On the other hand, transformation of hardened gypsum into hydroxyapatite (HA) by treatment in ammonium phosphate solution was found lately. In the present study, transformation of the 3DP gypsum block to HA was attempted. However, the fabricated 3DP block was soluble in water. To insolubilize, it was heated at 300°C for 10 min, and then, gypsum was transformed to calcium sulfate hemihydrate, $CaSO_4 \cdot 0.5H_2O$. The 3D block was immersed in 1*M* $(NH_4)_3PO_4 \cdot 3H_2O$ solution at 80°C for 1–24 h, and the transformation into HA within 4 h was ascertained. A heat-treated plaster of Paris (POP) block was also investigated for comparison. The unheated POP block consisting of gypsum dihydrate took 24 h to complete the transformation, while the heat-treated POP consisting calcium sulfate hemihydrate promoted the transformation into HA; but the transformed thickness in the block was less than the 3DP block. This is probably due to higher solubility of the hemihydrate than gypsum dihydrate. Accelerated transformation of the 3DP block was also caused by its porous structure, which enabled an easy penetration of the phosphate solution. With the present method, it is possible to transform the fabricated gypsum by 3D printing that is adaptive to the osseous defect into HA prostheses or scaffold. © 2006 Wiley Periodicals, Inc. J Biomed Mater Res Part B: Appl Biomater 80B: 386–393, 2007

Keywords: gypsum; hydroxyapatite; biocompatibility; hard tissue

INTRODUCTION

In the fields of orthopedics and oral surgery, common bone substitution materials are autograft, allograft, and xenograft. Hydroxyapatite (HA; $Ca_5(PO_4)_3OH$) is a main component of bone and teeth and is known as one of synthetic bone substitutes. HA has a superior biocompatibility and accelerates the new bone formation when it contacts with physiological fluid. It is rapidly integrated into the human bone and indistinguishable unions are formed.[1–3]

Calcium phosphate cements (CPCs), a new technology in craniofacial surgery, are an alternative HA bone substitutes. As a moldable treatment modality, CPCs can bond chemically to the host bone, restore contour, and augment the biomechanical properties of the injured or reconstructed region.[4] Barralet et al. reported that CPCs can be formed by the low-temperature process that may encourage biologically active organic compounds to be incorporated in the CPCs.[5]

For artificial bone, two types of HA, block and granular forms, have been developed. HA granules are considered to be easier to fill the defective area than the HA block because of the difficulties in trimming the HA block,[6] but it is limited within the small defect without load. Many attempts have been made to fabricate the HA artificial bone or scaffolds with desirable dimensions and internal architecture.[7] Three-dimensional printing (3DP) is a CAD/CAM built-up technique using ink-jet printing and is a promising method to fabricate three-dimensional solid model with any shape. By using 3D shape data of bone defect, it is possible to fabricate prostheses or scaffold adaptive to the defect shape. At present, commercially available 3DP system can fabricate only gypsum model and not for bioceramics. It is still difficult to find the effective binder to fabricate HA model. HA scaffolds were made indirectly by a negative mold and sintering process,[8] but sintering process requires high-temperature treatment, and it leads to a well-crystallized HA with a

Correspondence to: R. Lowmunkong (e-mail: ac_dent@hotmail.com or ac_dent@dent.osaka-u.ac.jp)

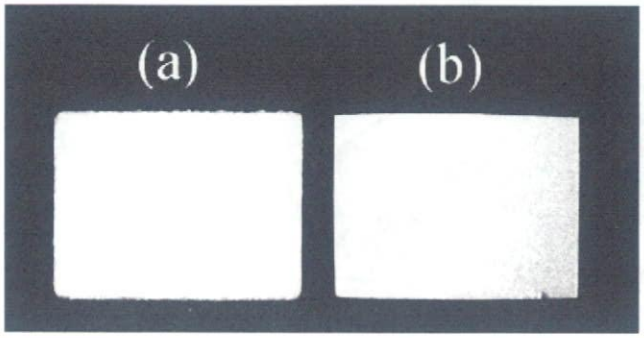

Figure 1. (a) 3DP block size of 20 × 15 × 4 mm^3; (b) plaster of Paris sample size of 20 × 15 × 4 mm^3.

low rate of biodegradation.[3,9] To avoid the disadvantages of sintering process of HA object fabrication, Tadic et al. had discovered a method to produce HA scaffold with interconnecting porosity without sintering.[10]

Plaster of Paris (POP; $CaSO_4 \cdot 2H_2O$) had also been used as a filling material for bone defect for long time.[11,12] As mentioned in the previous investigation of Frame, gypsum dihydrate can possibly be used as an alternative material to restore jaw bone defect. The result revealed corresponding progressive resorption rate with the new bone ingrowth in the *in vivo* experiment.[13] Sato et al. had investigated the morphologic sequence of the response to HA particle mixed with POP in the bone marrow of rabbit tibia. POP acts as an absorbable vehicle to HA particle; the mixture became viscous and formable. In addition, POP can be absorbed in relatively short time and does not interfere with bone healing process.[14]

Recently, Suzuki et al. reported that gypsum could be transformed into HA with preserving its original shape by the treatment in 1*M* ammonium phosphate solution at 100°C for 24 h.[15] If the gypsum bone or scaffold model with definite shape can be transformed into HA and the shape remains unchanged, the application of 3DP model to the osseous defects would be promising in the future.

The purpose of this study is to investigate the possibility of transformation of gypsum 3DP model into HA with preserving the original shape by treating it in the ammonium phosphate solution. Its transformation process was compared with a set POP, which is often used as a gypsum model material in dentistry. Product phase by the treatment of the 3DP model and POP was analyzed by X-ray diffraction (XRD). The crystal morphology of the treated 3DP specimen was observed by a scanning electron microscope (SEM).

MATERIALS AND METHODS

Fabrication of 3D Printing Model

Fifty pieces of simple rectangular (20 × 15 × 4 mm^3) blocks, as shown in Figure 1(a), were designed by CAD using software (FreeForm V.7 and PHANToM Desktop, SensAble Technologies, Woburn). The data was transformed to 3DP system [Figure 2(a)] (Z310, Z Corporation, Burlington) and fabricated. 3DP system fabricates complex 3D parts directly from the model designed by computer [Figure 2(b)]. During fabrication, a thin layer of powder (Powder; Z100, Z Corporation, Burlington) is spread on a piston plate and a print head deposits binder droplets (Binder ink; zb-7, Z Corporation, Burlington) in selective areas to create the model. After one layer is completed, the piston plate is lowered, and the lamination process is iterated until fabrication is completed. The layer thickness for fabrication was 0.08 mm, and mean diameter of gypsum grain was 30 μm.

3DP method enabled fabrication of models with any complicated shape. In this study, we also fabricate a mandibular model by 3DP technique. The CT scan data of mandible was transformed to STL data via software VG StudioMax (Volume Graphics, Heidelberg, Germany). From STL data, it was transferred to 3DP system, and model of mandible was fabricated.

We attempted to transform the 3DP block to HA by treating in ammonium phosphate solution. But, in our preliminary experiment, the 3DP blocks were found to be dissolved in water easily. Several methods were tried to find the way to insolubilize the block. The trials were made by changing the heating condition at several ranges of temperature in the drying oven (DX 300, Yamato, Tokyo, Japan).

Solubility test of various temperatures of heat-treated 3DP samples was investigated. The analysis of the 3DP samples included five groups of three samples: 3DP without any treatment, samples heat-treated at 100°C for 30 min, at 200°C for 30 min, at 300°C for 10 min, and at 300°C for 30 min. Each sample was soaked in 1 L of distilled water for 12 h, and calcium ion content in the solution was measured by ICP (inductively coupled plasma) optical emission spectroscopy (Optima 3000XL, PerkinElmer, Wellesley).

Preparation of Plaster of Paris Block

Plaster of Paris (POP, $CaSO_4 \cdot 0.5H_2O$; Maruishi Gypsum, Osaka, Japan) was mixed with water at *W/P* ratio of 0.50 to prepare 100 pieces of gypsum blocks ($CaSO_4 \cdot 2H_2O$) with the same size (20 × 15 × 4 mm^3) of the 3DP blocks and used as a control [Figure 1 (b)]. To compare the result with the heated 3DP block, the POP block was also heat treated in a similar method.

Treatment with Ammonium Phosphate Solution

Groups of 5 pieces of heat-treated 3DP rectangular blocks were immersed in 1 mol/L tri-ammonium phosphate solution prepared from a commercial reagent, $(NH_4)_3PO_4 \cdot 3H_2O$ (Wako Pure Chemical, Kyoto, Japan) at 80°C for 1, 2, 4, 6, 8, 12, and 24 h. After treated with the ammonium phosphate solution, the blocks were soaked and rinsed in distilled water and dried at room temperature (24°C).

Examination by XRD Analysis

To analyze the composition of the specimens, 3 to 5 pieces from each group of randomly selected 3DP and gypsum

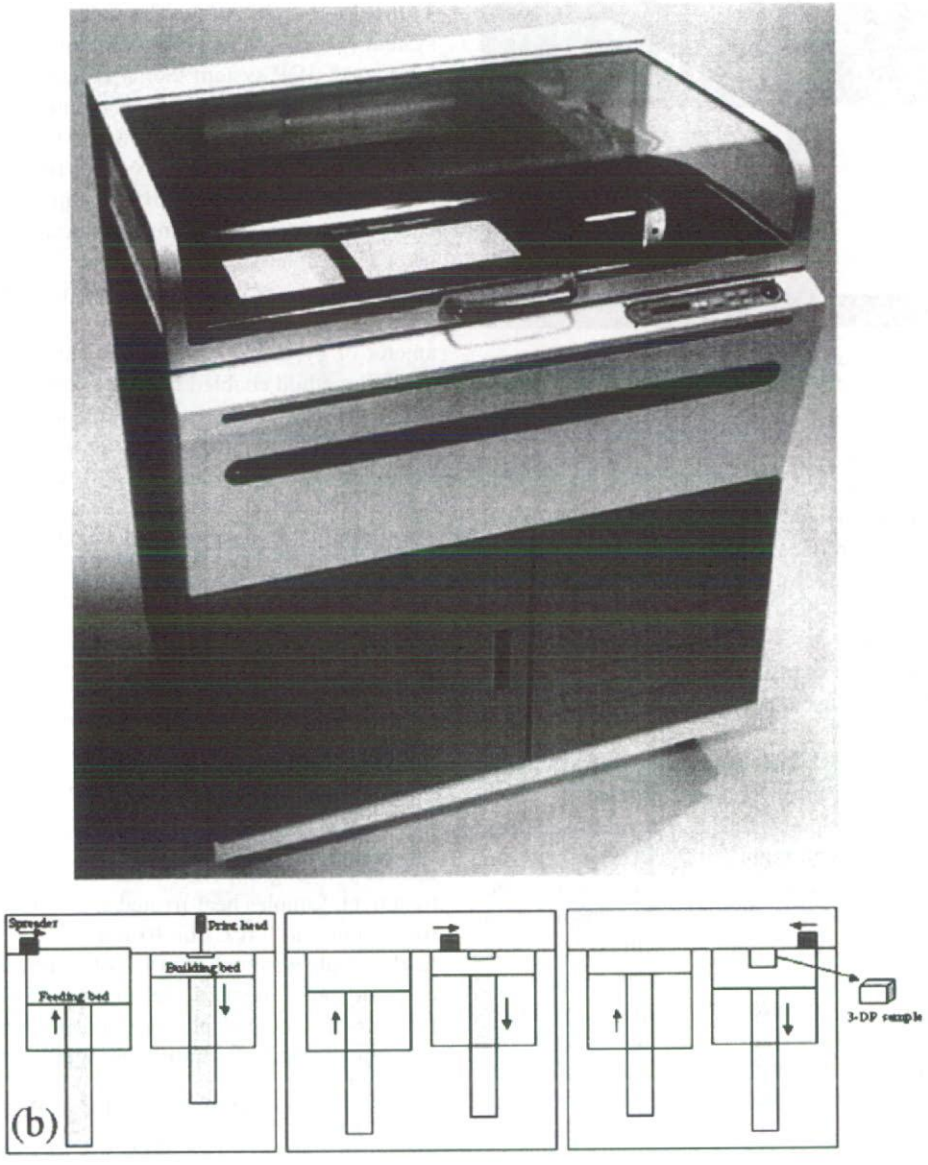

Figure 2. (a) 3DP machine (Z310, Z Corporation); (b) fabrication process of 3DP system.

blocks underwent XRD analysis before and after the treatment. In the analysis, pure hydroxyapatite powder (Taihei Chemical, Osaka, Japan) was used as a control. XRD pattern of the specimens were taken with a diffractometer with Cu Kα radiation generated at 40 kV/30 mA (RINT 2100, RIGAKU, Tokyo, Japan).

SEM Observation

The surfaces of specimens; untreated 3DP samples, 3DP samples treated in ammonium phosphate solution at 80°C for 12 and 24 h were observed by a field emission SEM (S-4300, Hitachi, Tokyo, Japan). The samples were randomly selected from the rest of samples that were not taken for XRD.

RESULTS

Insolubilization of 3D Printing Blocks by Heat Treatment

When the 3DP block was immersed in water, it was easily disintegrated as shown in Figure 3. It was also found to be easily disintegrated in the ammonium phosphate solution. To find the method to insolubilize the 3DP block, it was heat treated at various temperatures between 100 and 300°C. Solubility tests in water after heating were shown in Figure 4. As shown in Figure 4(c), the heat treatment at 300°C for 10 min yielded an optimum condition for insolublizing, though the color of 3DP block specimen became dark brown. The longer treatment time of 30 min at 300°C [Figure 4(d)] resulted in fragility of the specimen.